

BRAIN TUMOR CLASSIFICATION USING CNN FRAMEWORK

¹Hitesh Sharma, ² Bapuramji

^{*1&2}Department of Medical Research
Lokmanya Tilak Municipal Medical College, Sion Mumbai
Available online at: <http://www.ijcert.org>

Received: 20/07./2019,

Revised: 25/07./2019,

Accepted: 15/08./2019,

Published: 20/08./2019

Abstract: Brain tumour segmentation is considered a complex procedure in magnetic resonance imaging (MRI), given the diversity of tumour forms and the complexity of determining tumour location, size, and shape. Manual segmentation of tumours is a time-consuming task that is very sensitive to human error. Therefore, this study offers an automated approach that can detect tumour fragments and divide the tumour into all image slices in volume MRI brain scanners. First, a set of algorithms is used in the pre-processing phase to clean up and validate the collected data. Grey-Level Similarity Matrix Analysis and Analysis Of Variance (ANOVA) are used to obtain and select entities, respectively. Multilayer perceptron is accepted as a neural network classification, and a limited 3D window genetic algorithm is used to determine the location of abnormal tissue in MRI slices. Finally, active borderless 3D imaging is used to segment brain tumours using volume MRI exams. The experimental data set contains 165 patient images collected from the MRT unit of Al-Qadimiya University Hospital in Iraq. Tumour resection results achieved 89% _4.7% accuracy compared to manual procedures.

Key Words: Magnetic resonance imaging; modified gray level co-occurrence matrix, brain tumour classification; convolutional neural network; image classification.

1. Introduction

Brain tumours are less common than other tumours, such as brain and breast, but are considered important due to pathological effects and high morbidity. Accurate identification and differentiation of brain tumours and strokes can significantly affect clinical diagnosis, prognosis, and treatment.

The use of depleted uranium and other toxins in the First and Second Gulf Wars has increased the average number of annual cancer brain tumours and birth defects since 1990, the Iraqi Ministry of Health reports. The study was conducted in collaboration with MRI units, mainly in Iraqi hospitals. With the development of medical imaging technologies, the role of image processing has increased, and additional images can be obtained using a large number of acquisition techniques. As a result, image processing is

integrated into medical systems and is widely used in medicine, from diagnosis to treatment. Until now, diagnostic imaging has been a valuable tool in medicine. Standard medical imaging techniques, such as ultrasound, computed tomography, and magnetic resonance imaging (MRI), have significantly improved knowledge of anatomy and diagnosis in medical research. Among these medical technologies, MRI is considered to be the most useful and appropriate brain imaging technology. Tumours than other methods. MRI provides detailed information on the type, location and size of tumours non-invasively. In addition, MRI is more sensitive to local changes in tissue density. The spatial resolution of the scanning process, which is assigned a number to each pixel of the original image, has increased significantly in recent years. Standard MRI protocols are commonly used to generate multiple images of the same tissue after administration of parametric agents, including T1

weighting (T1-w), T2 weighting (T2-w), and fluid-reduced reverse recovery (FLAIR).), And with T1-weighted images with contrast enhancement (T1c-w). T1-w images are obtained by activating pure magnetization or proton T1 relaxation to recover 63% of the initial net magnetization after deactivation of the RF pulse from the MRI scanner. On the other hand, T2-w images are obtained during T2 relaxation, which is the time required for the net magnetization to decrease to 37% of the initial net magnetization. FLAIR is a special MRI scanner protocol that generates positive T2-w images by removing signals from cerebral edema and other highly water-rich structures such as cerebrospinal fluid (CSF).

Most brain tumours have hypo intensive intensity in T1-w images and hyper intensive in T2-w images. Therefore, T2-w images are commonly used to provide preliminary assessment, identify tumour types, and distinguish tumours from non-tissues. Contrast material is commonly used to increase the tumour boundary to surrounding normal brain tissue in T1-w images. This method cannot differentiate and detect tumour detection from T2-w and T1-w images due to its similarity to adjacent normal brain tissue. In clinical mode, T2-w is scanned as soon as the patient is placed to determine the location of the tumour. T1-w scanning is used before and after contrast administration to tumours with contrast enhancement. Axial T2-w scanning with FLAIR is used to show untreated tumours.

As the scanner's resolution improved, the thickness of the slices decreased, more and more pieces were made, and doctors needed more time to evaluate each patient from the image sets. Therefore, automatic tumour detection and segmentation has received considerable attention in the last two decades.

A particular challenge in imaging characteristics is the similarity of white matter tumours in the brain and the overlap of intensity distribution with gray matter. The specimen is visible at the boundary between the tumour and the surrounding tissue. Partial volumes (PV) are considered to be limiting properties formed by different types of tissues. The thickness of the image pieces (from 5 to 7 mm) creates significant PV effects, in which individual pixels of the image describe more than one type of tissue. As a result, peripheral tumour regions are incorrectly classified. This event is common in T2-w movies. A similar problem occurs at the outer edge of the brain, where CSF and gray matter overlap with the image pattern. This condition can cause an image intensity that distorts the presence of the tumour.

In recent decades, the number of studies devoted to the automated segmentation of brain tumours has grown rapidly due to advances in medical imaging. Active contours or snakes are very important for differentiating brain tumours. These tools are ideal for demarcating the tumour and surrounding tissues. This approach allows the separation,

alignment and monitoring of anatomical areas using anatomical and biological knowledge of the location, size and shape of anatomical areas. Active contours are defined as curves or moving surfaces under the influence of weighted internal and external forces. Internal forces are responsible for the sensitivity to curvature, while external forces push and pull curves toward the boundaries of the anatomical zone.

In general, the active contour design suffers from the problem of initial shape detection and leakage at the fuzzy edges. Most of the proposed approaches to identifying and segmenting brain pathologies are limited by (i) computer complexity; (ii) lack of complete automation due to the variability of brain tumours; (iii) the problem of shape and blurred edge initialization.

To overcome these problems, we have developed a fully automated method for identifying the initial shape and differentiation of brain tumours using an active three-dimensional structure without borders (3DACWE). In addition, we compared the details of 2D and 3D.

Our system is based on the use of a single MRI (T2-w image) in axial view to detect brain abnormalities (such as sagittal and coronal images) instead of multimodal MRI. Using simple symmetry of the brain structure, the system searches in parallel for different regions that correspond to its reflection in the opposite hemisphere of the brain. This method automatically starts the splitting process. As a result, the proposed system is fully automated and independent of atlas registration to avoid erroneous registration processes that directly affect the accuracy of tumour resection. Before such a strategy, the skull removal step is not necessary.

The remaining sections of this paper are organized as follows: in Section 2, the proposed method is explained; in Section 3, experimental results are discussed while describing how to locate and identify the tumor; and in Section 3, the conclusions are given.

2. Related Works

During the DIP, the images are captured and processed to distribute and retrieve the required information. Digital image division refers to the division into several categories. Associated segmentation is needed to provide a larger and clearer representation of image alternatives to detect and analyze abnormalities in the brain. In recent decades, researchers have proposed several segmentation and detection algorithms. Threshold-based segmentation, region-based segmentation, edge detection, region segmentation and convergence, statistical clustering model (CSM), and artificial neural network (ANN) are the most commonly used detection techniques.

The threshold method is effective in the general technique of brain image segmentation and image banalization. The threshold cellar, however, can be used in conjunction with other methods such as classification,

grouping, ANN. Different ash levels. It depends on the separation of pixels in different classes according to the gray level of the pixels. Brain MRI image pixels can be identified as areas with a discrete gray scale range. The main difficulty is that it cannot be used for multichannel images. In a regional partition (also called an analogy partition), large areas are made up of pixels or subsets Zones according to predefined criteria.

This technique starts with a set of "seed" dots and generates regions from these dots by connecting each seed to adjacent pixels that have the same meaning as the seed. The disadvantages of using this method are the high calculation costs and the manual interaction required to select the starting points. In addition, it is very sensitive to noise. The growth and division of the region is a special case of the region's growing technology. The main purpose of separating and merging zones is to separate the homogeneity of the image. The splitting method is used if, after applying the region augmentation technology, the region meets the homogeneity criteria, then four regions of the region are obtained. The main disadvantage of this technique is the flight to the borders.

Edge segmentation focuses on identifying texture and using image value breaks to separate regions. The main limitation of this method is that it is not possible to divide the given image into a blurred or very complex image. Classification methods require appropriate pixel classification for training data. The most commonly used classifiers are K-nearest neighbour (KNN), maximization of expectations (EM), etc. Effective classification and training data take time and require specific results. The KNN algorithm is a parameter-free method based on the distance function (Euclidean distance) and uses the voting function used for the nearest K neighbours. KNN demonstrates high accuracy and stability RM images than other classifiers. This algorithm is too large to implement, and in addition, real-time image segmentation is managed by KNN because it is executed faster. The disadvantage of using this algorithm is that it is possible to make the wrong decision when the obtained neighbours belong to the second class.

The support vector machine (SVM) operates on the basis of monitored classification and training models and aims to reduce the limits of generalization errors. It offers better generalization performance and works with more functionality space. However, its implementation is long and suitable for tumour classification. Among clustering methods, K stands for clustering algorithm, FCM clustering algorithm, and expectation maximization (EM) algorithm are the most common ways to detect brain tumours. Clustering is a method of dividing a data set into a certain number of groups. The K-means clustering algorithm is an unsupervised algorithm that separates k into groups based on attributes /

attributes (k is a positive integer). It is a very simple clustering algorithm designed to create a closed cluster that works well for small data. It works faster than hierarchical grouping when the number of variables is large. However, the disadvantages of this algorithm are that the value of K is difficult to estimate and does not work well in the global cluster. In addition, with different sizes and densities, the performance of this algorithm is negligible.

Fuzzy C - A soft clustering technique in which each pixel belongs to two or more clusters. Describes the distance between cluster centres and models of the total objective function. It only takes into account image intensity values and does not filter, which offers high noise immunity and better compartment quality. There is a K-tool and an FCM algorithm that performs the initial resection and performs additional segmentation in the FCM image, and an accurate segmented tumour is detected by the FCM technique by precisely selecting clusters. Traditional FCM is limited in its sensitivity to noise, but immunity to K noise implies clustering. Prior to dissection, there must be a precise determination of the threshold, as it is difficult to complicate the structure of the brain. ANN is currently a very promising method for tumour detection and classification. ANN is divided into two parts: Feed Forward Neural Network (FFND) and Feed-Backward Repeat Network or Neural Network (FBNN). ANN technique provides stable parallelism and fast calculation. However, the creation of input images takes a long time, and some of the information must be known in advance. From the above discussions, it can be argued above that there is less ideal technology. But in order to create an optimal result in this area, we have identified the limitations of the individual methods described here.

K-Means and Fuzzy C-Means Clustering Algorithm:

K-Mean Clustering Algorithm: The K-Mean clustering algorithm is a very simple unattended learning algorithm. It provides a very simple way to classify the given data into several sets, that is, in data sets such as $x_1, x_2, x_3, \dots, x_n$ are classified into K clusters. The main idea of this algorithm is to define K centres, one for each cluster. Cluster centres K must be chosen at random. Distance measurement plays a very important rule in the operation of this algorithm. Various distance measurement methods are available for this algorithm, such as Euclidean distance, Manhattan distance and Chebichev distance. However, the choice of the optimal method for calculating the distance depends entirely on the type of data we use for the cluster. However, we use the Euclidean distance as a distance metric because it is fast, powerful, and easy to understand. The classic step-by-step grouping algorithm for features K is described as follows.

Algorithm 1 K-means clustering algorithm.

Assume that, $X = x_1, x_2, x_3, \dots, x_n$ be the set of data points and $V = v_1, v_2, v_3, \dots, v_c$ be the set of centres

- 1: Define number of clusters $0 < K < \infty$.
- 2: Randomly, define cluster centres $0 < c < \infty$.
- 3: Calculate the distance between each data point and cluster centres.
- 4: Data point is assigned to the cluster centre whose distance from the cluster centre is minimum of All the cluster centres.

Relevancy between Brain Tumour and Genes

As discussed in the last section, mutations in certain types of genes determine cancer. In various studies, a relationship was found between the level of mutations and the type of brain tumour in the genes, Tumour protein 53 (TP53) is involved in DNA and apoptosis. Tp53 levels are highly abnormal in high-grade gliomas, and mutations have been detected in more than 80% of tumours. The retinoblastoma gene (RB1) is a tumour suppressor gene. The RB1 mutation is present in approximately 75% of brain tumours and is more significant in glioblastoma. EGFR is a transmembrane receptor in the tyrosine kinase (RTK) receptor family. EGFR mutation leads to increased cell cycle proliferation and tumour cell survival. It is commonly associated with primary glioblastomas and accounts for approximately 40% of the mutations that cause it. PTEN is a tumour suppressor gene and causes 15 to 40% of the mutations found in primary glioblastomas. With glioblastoma apathy, the mutation rate can reach 80%. IDH1 and IDH2 are enzymes that regulate the citric acid cycle. Their mutations inhibit the activity of enzymes. In general, the IDH1 mutation is less common in patients with primary glioblastoma (5%) and higher in patients with high-grade glioblastoma (70-80%). IDH2 mutations are commonly found in oligodendroglioma tumours. Coding of chromosomes 1p and 19q deletes the oligodendroglioma line and is mainly observed in anaplastic oligodendroglioma (20-30%), oligodendroglioma (30-50%), anaplastic oligodendroglioma's (60%) and oligodendroglioma's (60%). 1p / 19q helps in the prediction and evaluation of treatment. MGMT is another DNA repair gene for which glioblastomas have been detected in 35 to 75% of cases. BRAF is a proto-oncogene encoded as a BRAF protein involved in the cell proliferation cycle, apoptosis, and therapeutic evaluation. BRAF mutations are most common in pilocytic astrocytomas (65-80%), pleomorphic xanthocystoma (approximately 80%) and gangliogliomas (25%) [26]. X-linked thalassemia mental retardation syndrome (ATRAX) is a protein that encodes a protein and is associated with TP53 and IDH1 mutations. It is used as a prognostic indicator when tumours have an ANIDH1 mutation and can differentiate tumours of oligodendroglioma origin.

Imaging Modality

Medical imaging techniques help doctors, physicians, and researchers look into the human body and analyse internal activities without incisions. Cancer diagnosis, grade assessment, treatment response assessment, patient prognosis, and surgical planning are key stages and challenges in cancer treatment. There are many medical imaging techniques used by hospitals around the world for a variety of treatments. Brain imaging techniques can be divided into two types: namely, structural and functional imaging. Structural imaging involves a variety of functions related to brain structure, tumour location, damage, and other brain disorders. Functional imaging techniques detect metabolic changes, fine-grained damage, and visualize brain function. Visualization of this activity is possible due to changes in the metabolism of a certain part of the brain, which is reflected in the scan. CT and MRI are used for the analysis of brain tumours, and they can detect various cross-sections of the body without surgery

3. Materials and Methods

Image Database: The image database, which is presented as a set of parts, contains 3064 T1-weighted, contrast-enhanced MRI images obtained from Tianjin Medical University, Nanfang Hospital, and China General Hospital from 2005 to 2010. It was first published online in 2015 and the last revised version was prepared in 2017. There are three types of tumours: meningioma (708 images), glioma (1426 images) and pituitary tumour (930 images). All images were obtained from 233 patients on three flights: sagittal (1,025 images), axial (994 images), and coronal (1,045 images). Examples of different types of tumours as well as different planes are shown in Figure 1. Tumours are marked with a reddish shape. The number of images varies.

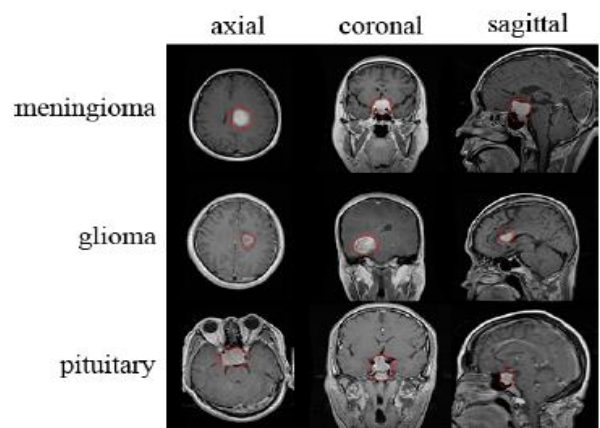


Figure 1. Imaging of normal magnetic resonance imaging (MRI) images showing different types of tumours in different planes. In the pictures, the tumour is marked in red. An example of each type of tumour is given in each plan.

Image Pre-Processing and Data Augmentation: Database magnetic resonance images come in a variety of sizes and are provided in int16 format. These images represent the network input layer, so they are normalized and resized to 256×256 pixels.

In order to augment the dataset, we transformed each image in two ways. The first transformation was image rotation by 90 degrees. The second transformation was flipping images vertically. In this way, we augmented our dataset three times, resulting in 9192 images.

Network Architecture: To enlarge the dataset, we modified each image in two ways. The first transformation is to rotate the image 90 degrees. The second transformation consists of the vertical rotation of the images. So, we tripled our dataset to get 9,192 images. Network architecture: Tumour classification was performed using CNN developed by Matlab R2018a (The Math works, Natick, MA, USA). As shown in Figure 2, the network architecture consists of an input, two main blocks, a classification block, and an output. The first main block, block A, consists of a convolutional layer, which gives the image twice as much output as the provided output. The convolutional layer is followed by a rectified linear unit activation layer (coil) and a stop layer. This block also has a maximum grouping layer that outputs the output half of the input size. The second block, block B, differs from the first convolution in a layer whose output is equal to the input of that layer. The classification block consists of two fully connected layers (FC), the first of which represents the flat result of the final maximum grouping layer, while the number of hidden units in the second FC layer is equal to the tumor class. The whole network structure consists of an input layer, two A blocks, two B blocks, a classification block and an output layer; There are a total of 22 layers, as shown in Table 1

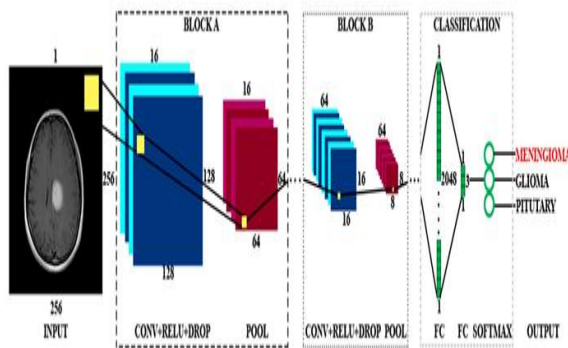


Figure 2. Schematic representation of convolutional neural network (CNN) architecture containing the input layer, two Blocks A, two Blocks B, classification block and output. Block A and Block B differ only in the convolution layer. Convolution layer in Block A gives an output two times smaller than the input, whereas the convolutional layer in Block B gives the same size output as input.

Table 1. New CNN architecture. All network layers are listed with their properties.

Layer No.	Layer Name	Layer Properties
1	Image Input	256 × 256 × 1 images
2	Convolutional	16 5 × 5 × 1 convolutions with stride [2 2] and padding 'same'
3	Rectified Linear Unit	Rectified Linear Unit
4	Dropout	50% dropout
5	Max Pooling	2 × 2 max pooling with stride [2 2] and padding [0 0 0 0]
6	Convolutional	32 3 × 3 × 16 convolutions with stride [2 2] and padding 'same'
7	Rectified Linear Unit	Rectified Linear Unit
8	Dropout	50% dropout
9	Max Pooling	2 × 2 max pooling with stride [2 2] and padding [0 0 0 0]
10	Convolutional	64 3 × 3 × 32 convolutions with stride [1 1] and padding 'same'
11	Rectified Linear Unit	Rectified Linear Unit
12	Dropout	50% dropout
13	Max Pooling	2 × 2 max pooling with stride [2 2] and padding [0 0 0 0]
14	Convolutional	128 3 × 3 × 64 convolutions with stride [1 1] and padding 'same'
15	Rectified Linear Unit	Rectified Linear Unit
16	Dropout	50% dropout
17	Max Pooling	2 × 2 max pooling with stride [2 2] and padding [0 0 0 0]
18	Fully Connected	1024 hidden neurons in fully connected (FC) layer
19	Rectified Linear Unit	Rectified Linear Unit
20	Fully Connected	3 hidden neurons in fully connected layer
21	Softmax	softmax
22	Classification Output	3 output classes, "1" for meningioma, "2" for glioma, and "3" for a pituitary tumor

Training network: We used the k-fold cross-validation method to test the network performance. Two different approaches have been introduced and both have ten times cross-validation. The first approach is to randomly divide the data into 10 equal parts so that each tumour category is the same, and this is called cross-validation at the entry level. The second approach is to randomly divide the data into about 10 equal parts, where only one dataset of the same subject can be found. Therefore, each set contains data from specific subjects regardless of the tumour class, known as subject cross-validation. The second approach has been used to test the generalization of the network in medical diagnostics. The ability to generalize in clinical practice refers to the ability to make a diagnosis based on data obtained from subjects who are not observable during the training process. Therefore, the observations of the individuals included in the training kit should not be visible in the test kit. If this is not the case, a complex stroke may choose a confusing link between the identification of participants and the diagnostic status and lead to an unrealistically high level of predictive accuracy. To compare our network performance with other sophisticated methods, we tested our network without k-fold cross-validation (test). Of all the above methods, two data components, two for validation and six for training were used for testing. Simple and augmented data sets were tested using all methods.

The network is created using the Adam optimizer, with a mini-batch size of 16 and data mixing at each iteration. The start-stop situation, which affects the stopping of the networking process, corresponds to the era. In particular, when the damage starts to increase, an era is set for the training process to be completed later. The

normalization factor was set at 0.004 and the initial learning rate was 0.0004. The weight of convolutional platelets was initiated using the initiator Glorot, also known as the initiator Xavier.

The training process was stopped when the validation set losses were 11 times greater than or equal to the previous minimum losses. This network is set up and tested in a single graphics processing unit (GPU), CUDA device, GeForce GTX 1050 Ti.

4. Conclusions

The visual diagnosis of MRI images is highly dependent on subjective competence and the physician. The proposed method reduces the assessment time of the clinician from 3 to 5 hours to 5 to 10 minutes without significantly reducing the accuracy of the diagnosis. Of course, the proposed method can detect and MRI segment (tumour) of brain abnormality on T2-w, T1-w, T1c-w and FLAIR images. The 3DACWE segmentation technique reduces manual entry, offers faster operation, and has higher accuracy compared to manual segmentation estimated using the data sets AI-Kadamiya and BRATS 2013. Because we conclude that the 3DACWE method is effective in differentiating brain tumours the procedure takes into account not only the local characteristics of the tumour, such as gradients, but also based on general characteristics, such as intensity, shape length, and area length. 3DACWE excretes brain tumours very slowly, although the accuracy obtained is high compared to other segmentation methods. A large number of MRI slices with a resolution of 512 to 512 pixels with a high number of repetitions were used to obtain the slow and required processing accuracy.

References

1. Selkar, R.G.; Thakare, M. Brain tumour detection and segmentation by using thresholding and watershed algorithm. *Int. J. Adv. Inf. Common. Technol.* 2014, 1, 321–324.
2. Borole, V.Y.; Nimbhore, S.S.; Kawthekar, D.S.S. Image Processing Techniques for Brain Tumor Detection: A Review. *Int. J. Emerg. Trends Technol. Comput. Sci.* 2015, 4, 28–32.
3. Mustaqeem, A.; Javed, A.; Fatima, T. An efficient brain tumor detection algorithm using watershed & thresholding based segmentation. *Int. J. Image Graph. Signal Process.* 2012, 4, 34–39.
4. Kaur, H.; Mittal, M. Region Based Image Segmentation for Brain Tumor Detection. *Int. J. Eng. Manag. Res.* 2016, 6, 31–34.
5. Sinha, K.; Sinha, G. Efficient segmentation methods for tumor detection in MRI images. In *Proceedings of the IEEE 2014 IEEE Students' Conference on Electrical, Electronics and Computer Science*, Bhopal, India, 1–2 March 2014; pp. 1–6.
6. Karkavelas, G.; Tascos, N. Epidemiology, histologic classification and clinical course of brain tumours. In *Imaging of Brain Tumors with Histological Correlations*; Springer: Heidelberg, Germany, 2002; pp. 1–10.
7. Nabizadeh, N.; Kubat, M. Brain tumours detection and segmentation in Mr Images: Gabor wavelet vs. Statistical features. *Comput. Electr. Eng.* 2015, 45, 286–301. [CrossRef]
8. Hasan, A.; Meziane, F. Automated screening of mri brain scanning using grey level statistics. *Comput. Electr. Eng.* 2016, 53, 276–291. [CrossRef]
9. Dougherty, G. *Digital Image Processing for Medical Applications*; Cambridge University Press: Cambridge, UK, 2009.
10. Mechtler, L. Neuroimaging in neuro-oncology. *Neurol. Clin.* 2009, 27, 171–201. [CrossRef] [PubMed]
11. World Health Organization—Cancer. Available online: <https://www.who.int/news-room/fact-sheets/detail/cancer>. (accessed on 5 November 2019).
12. Priya, V.V. An Efficient Segmentation Approach for Brain Tumor Detection in MRI. *Indian J. Sci. Technol.* 2016, 9, 1–6.
13. Cancer Treatments Centers of America—Brain Cancer Types. Available online: <https://www.cancercenter.com/cancer-types/brain-cancer/types> (accessed on 30 November 2019).
14. American Association of Neurological Surgeons—Classification of Brain Tumours. Available online: <https://www.aans.org/en/Media/Classifications-of-Brain-Tumors> (accessed on 30 November 2019).
15. DeAngelis, L.M. Brain Tumors. *New Engl. J. Med.* 2001, 344, 114–123. [CrossRef]